Outage and Diversity Analysis of Underlay Cognitive Mixed RF-FSO Cooperative Systems

Hamid Arezumand, Hossein Zamiri-Jafarian, and Ehsan Soleimani-Nasab

***Abstract*—We investigate the performance of asymmetric radio frequency (RF) and free-space optical (FSO) dual-hop cognitive amplify-and-forward relay networks where RF links are subject to independent and nonidentically distributed Nakagami-*m* fading. We consider that the RF link transmitter and receiver are secondary users of an underlay cognitive network. Specifically, the transmit power conditions of the proposed spectrum-sharing network are governed by either the combined power constraint of the interference on the primary network and the maximum transmission power at the secondary network, or the single power constraint of the interference on the primary network. Also, we consider a double generalized gamma fading channel with pointing error and both heterodyne and intensity modulation/direct detection methods in the FSO link. The closed-form and asymptotic expressions of outage probability for this system are calculated for fixed gain and channel-state-information-assisted relaying techniques. It is demonstrated that the diversity order is a function of the fading severity of the RF link, turbulence parameters of the FSO link, and pointing error, regardless of the interference channel parameter of the primary user. However, the coding gain is impressed by the interference link parameter and RF-FSO links parameters. The diversity-multiplexing trade-off analysis is done for this network, where we show that this trade-off is independent of the primary network.**

***Index Terms*—Amplify-and-forward; Cognitive radio network; Double generalized gamma; Dual-hop relaying; Free-space optical communications; Outage probability; Underlay spectrum sharing.**

I. Introduction

The development of current and future wireless applications is being restricted by resource and energy limitations. The demand for additional spectrum is even more problematic since it is growing faster than the technology that is able to increase the spectrum efficiency. An intelligent cognitive radio technology together with dynamic spectrum access illustrates a novel way to solve the above-mentioned problems [1]. More specifically, in the underlay spectrum access scheme, secondary users (SUs) can utilize the spectrum holes of primary users (PUs) as long as the interference power they impose on the PUs remains below specific thresholds [2]. On the other hand, in order to increase the transmission rate of wireless users, the concept of cooperative communication has received significant attention in recent years. In fact, many cooperative strategies have been proposed in the literature based on different relaying techniques. However, the two most widely used protocols are amplify-and-forward (AF) and decode-and-forward (DF). The AF relaying schemes have low complexity and are suitable to be deployed in future wireless systems. Cooperative spectrum sharing is a promising approach that merges two main concepts of wireless communications. Cooperative diversity enhances the reliability of communications, and cognitive radio improves the efficiency of spectrum utilization.

On the other hand, free-space optical (FSO) systems provide high data rates, low-cost deployment, and superior security in the unregulated spectrum [3]. They can be employed together with RF technology to fill the last mile connectivity gap that exists between the fiber-optic-based backbone network and the RF access network. In mixed RF-FSO systems, RF and FSO links are being used in a dual-hop configuration [4,5]. To model the turbulence effect of the FSO link, various models have been proposed, such as the log-normal model, the gamma–gamma (G^2) model, and the double Weibull model [6].

In the literature, performance analyses of mixed dual-hop AF RF-FSO relaying systems were done for various conditions [4,7–18], where both intensity modulation/direct detection (IM/DD) and heterodyne systems are assumed under the consideration of AF relaying [4,7–18]. In Ref. [7], the RF-FSO network was introduced for the first time. The outage probability (OP) and bit error rate of this system were derived for Rayliegh/G^2 fading with the assumption of pointing error and both IM/DD and heterodyne detection methods [10], and the authors of Refs. [8,9] extended this result, assuming the availability of outdated CSI in a multiple relay system. The authors of Ref. [11] presented a performance analysis of a relay network by considering Malaga distribution for the FSO link.

Manuscript received April 14, 2017; revised July 12, 2017; accepted July 19, 2017; published September 29, 2017 (Doc. ID 292527).

H. Arezumand and H. Zamiri-Jafarian (e-mail: hzamiri@um.ac.ir) are with the Electrical Engineering Department, Ferdowsi University of Mashhad, Mashhad 9177948974, Iran.

E. Soleimani-Nasab is with the Faculty of Electrical and Computer Engineering, Graduate University of Advanced Technology, 7631133131 Kerman, Iran.

https://doi.org/10.1364/JOCN.9.000909

The fading distribution of the RF link was extended to Nakagami-m fading, Rician fading, and $\kappa-\mu$ and $\eta-\mu$ distributions in Refs. [12,13,15] and [14], respectively. In Ref. [19], the authors considered $\eta-\mu$ and Malaga distributions for the mixed RF-FSO relaying system. Performance analyses of fixed gain and CSI-assisted relaying scenarios were done while multiuser selection was performed at the source node.

Though G^2 became the widely used distribution for channel modeling in FSO systems, G^2 distribution does not completely match with experimental data, particularly in the tails [20]. A new general statistical model, called double generalized gamma (DGG) distribution, has been recently proposed in Ref. [20], where irradiance fluctuations are given by the production of small-scale and large-scale fluctuations, both of which are functions of the generalized gamma distribution. This model can be used to accurately describe the signal propagation under all conditions, (i.e., from weak to strong turbulence conditions) added to the fact that it generalizes other distributions.

The turbulence distribution of the FSO link has been generalized to DGG turbulence in Ref. [4], where the RF link was Rayleigh distributed, and in Ref. [21], where the RF link was Nakagami-m distributed and the impact of cochannel interference was considered as well. In Ref. [22], the authors considered a multiple input multiple output (MIMO) system for the RF link where space–time block coding was used. The authors of Ref. [19] extended these results for multi-user relaying systems, while power allocation and security-reliability analysis were considered in Refs. [23] and [24], respectively. Subsequently, the authors of Refs. [16–18] considered an underlay cognitive radio network (CRN) for the RF link where the PUs share their spectrum with the secondary network (SN) on the condition of no harmful interference to the primary network (PN). Therefore, the transmit power of the SUs was restricted to a predefined value, which was called the interference temperature (IT). In Refs. [16,17], performance analysis was done for variable and fixed gain relaying, respectively, where the RF-FSO links were experiencing Rayleigh fading/G^2 turbulence distributions. The authors of Ref. [18] considered a mixed RF-FSO underlay cognitive system where the relay and the PU were equipped with multiple antennas. They supposed Rayleigh and G^2 distributions for the RF and FSO links, respectively, and multiuser selection at the source and the destination was considered, while the interference caused by the PU to the SU was considered, too. Moreover, interference cancelation methods were used, the CSI-assisted relaying technique was employed, and tight upper-bound values on the OP and diversity order were obtained.

While all of the pervious works on RF-FSO systems [16–18] substantially provide a good understanding of CRNs, most of them assumed Rayleigh fading channels for the RF link. This may not be useful in a wide range of fading scenarios that are typical in realistic wireless relay applications. From a realistic point of view, the choice of Nakagami-m fading is to characterize more versatile fading scenarios that are more or less severe than Rayleigh fading via the m fading parameter, which includes the Rayleigh fading ($m=1$) as a special case. Furthermore, PUs and SUs are often far from each other; as such, independent and nonidentically distributed (i.n.i.d.) fading is assumed with distinct fading parameters in the links.

Motivated by the abovementioned limitations of Refs. [16–18], we herein pursue a detailed and generalized performance analysis of mixed RF-FSO cognitive AF relaying systems. The paper contributions can be summarized as follows:

- The OP of the underlay cognitive RF-FSO relaying system is achieved by assuming i.n.i.d. Nakagami-m fading for the RF links and DGG turbulence for the FSO link that includes G^2 turbulence for both fixed gain and CSI-assisted relaying techniques. We consider two power constraint strategies in a cognitive RF-FSO system.
- In order to get some additional insight into the impact of system parameters, the asymptotic expression of the OP for the high signal-to-noise ratio (SNR) is determined. Subsequently, it has been shown that the diversity order of a secondary network strictly depends only on the fading severity of the RF link, the turbulence parameters of the FSO link, and the pointing error, and is independent of the PU parameters. Additionally, the coding gain is a function of both the interference link parameter and two secondary hops.
- Diversity-multiplexing trade-off analysis is done for this CRN. It has been proved that the diversity-multiplexing trade-off is independent of the primary network. Furthermore, the key network parameters such as fading parameters of RF and FSO links and the distance between the secondary source and the PU are extracted.

The rest of the paper is organized as follows. Section II introduces the system model and fading characteristics. In Sections III and IV, we derive new expressions for the OP of the AF relay, considering both transmission constraints, and simplify them for the high-SNR asymptotic regime. Section VI presents numerical results, while Section VII concludes the paper.

Notation: Throughout this paper, we use $f_h(\cdot)$ and $F_h(\cdot)$ to denote the probability density function (PDF) and cumulative distribution function (CDF) of a random variable (RV) h, respectively. $\Gamma(n)=\int_0^\infty e^{-t}t^{n-1}\mathrm{d}t$ is the gamma function ([25], Eq. (8.310.1)), $\Gamma(n,x)=\int_x^\infty e^{-t}t^{n-1}\mathrm{d}t$ is the upper incomplete gamma function ([25], Eq. (8.350.2)), and $\Upsilon(n,x)=\Gamma(n)-\Gamma(n,x)$ is the lower incomplete gamma function. Furthermore, $G_{\cdot\cdot}^{\cdot\cdot}[\cdot]$ and $H_{\cdot\cdot\cdot\cdot}^{\cdot\cdot\cdot\cdot}[\cdot]$ denote the Meijer G-function and the extended generalized bivariate Fox H-function (EGBFHF), which are explained in [25], Eq. (9.301), and [26], Eq. (1), respectively. $[x]_p$ shows a vector with identical values equal to x and length p. Assuming that X is a RV, $\bar{X}$ is the denoted expected value of X (i.e., $\mathbb{E}[X]$). In the following, $\Delta(.:.)$, $\bar{\Delta}(.:.)$, and $\bar{\Delta}(.,.,.)$ are respectively defined as

$$\Delta(j{:}x) \triangleq \frac{x}{j}, \ldots, \frac{x+j-1}{j},$$
$$\bar{\Delta}(j{:}x) \triangleq \frac{x+j-1}{j}, \ldots, \frac{x}{j},$$
$$\bar{\Delta}(r,j,x) \triangleq \Delta\left(r, \frac{x+j-1}{j}\right), \ldots, \Delta\left(r, \frac{x}{j}\right).$$

II. System Model

We consider a CRN where the PU shares the licensed spectrum with the SU in the same region. As shown in Fig. 1, the SN consists of one source S, one relay R, one destination D, and the PN has one receiver P. The SUs use the given spectrum with the underlay approach, which means that any SU is allowed to use the spectrum only with the condition that no harmful interference to the PU has been guaranteed [27,28]. We assume that each node has a single antenna and operates in half-duplex mode. h_{SP}, h_{SR}, and h_{RD} are channel coefficients of $S \to P$, $S \to R$, and $R \to D$ links, respectively.

In this paper, we consider both fixed gain and CSI-assisted AF relaying techniques. In the first step of transmission, the RF modulated signal is transmitted from S to R via the RF link. The received signal at R can be written as

$$r_R = h_{SR}s + n_R, \tag{1}$$

where h_{SR}, s, and n_R are, respectively, the source to relay channel coefficient, the transmitted signal from S with average power $(\mathbb{E}[|s|^2] = P_s)$, and the additive white Gaussian noise (AWGN) with zero mean and variance N_R. The received signal at R is amplified with a proper gain G. In the CSI-assisted relaying technique, the relay amplification gain is defined as $G = 1/\sqrt{P_s|h_{SR}|^2 + N_R}$. In the fixed gain relaying technique, $G = 1/\sqrt{P_s\mathbb{E}[|h_{SR}|^2] + N_R}$. Using the subcarrier intensity modulation technique, removing the dc bias and converting the optical signal to the electrical one at D, the received signal at the destination can be written as

$$r_D = (\eta h_{RD})^{\frac{r}{2}} G r_R + n_D, \tag{2}$$

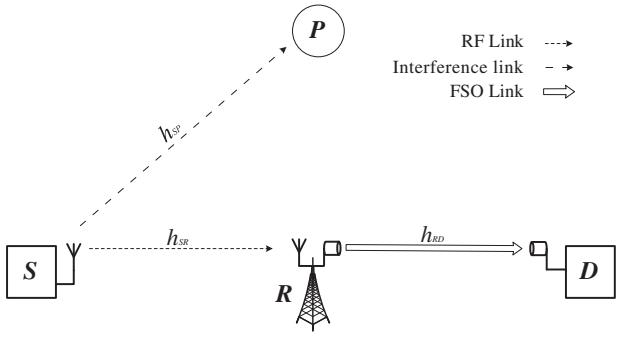

Fig. 1. System model of the cognitive RF-FSO transmission system.

where η is the electrical-to-optical conversion ratio, h_{RD} is the relay to destination channel coefficient, and n_D is the AWGN with zero mean and variance N_D, while r represents the detection method in the receiver ($r = 1$ represents heterodyne detection and $r = 2$ shows IM/DD) [21].

A. RF Link

We suppose h_{SP} and h_{SR} are RF links that undergo i.n.i.d. Nakagami-m fading; therefore, $|h_{SP}|^2$ and $|h_{SR}|^2$ are gamma distributed with fading severity parameters m_{SP} and m_{SR}, mean powers Ω_{SP} and Ω_{SR}, and finally scale parameters $a_{SP} = m_{SP}/\Omega_{SP}$ and $a_{SR} = m_{SR}/\Omega_{SR}$, respectively. The PDF and CDF of the gamma distribution are given respectively by [29], Eq. (2.21). We have

$$f_{|h|^2}(\gamma) = \frac{a^{m_{RF}}\gamma^{m_{RF}-1}}{\Gamma(m_{RF})} \exp(-a\gamma), \tag{3}$$

$$F_{|h|^2}(\gamma) = \frac{\Upsilon(m_{RF}, a\gamma)}{\Gamma(m_{RF})}, \tag{4}$$

where $a = m_{RF}/\Omega$, while m_{RF} is the severity parameter and Ω represents the average SNR per symbol.

The transmit power of S is limited to the maximum tolerable interference power of PN (i.e., Q). Let SUs also have a maximum transmit power constraint $P_{\max}$; therefore, the transmit power of S can be written as $P_s = \min(P_{\max}, Q/|h_{SP}|^2)$ [27]. The CSI of the interference link is obtained by S with many feasible methods, such as direct link [30] or channel reciprocity property of link [31]. Therefore, the SNR at R is $\gamma_R = \min(\bar{\gamma}_P|h_{SR}|^2, \bar{\gamma}_Q|h_{SR}|^2/|h_{SP}|^2)$, where $\bar{\gamma}_Q = Q/N_R$ and $\bar{\gamma}_P = P_{\max}/N_R$. In the other strategy, only the IT power constraint is considered for S. The transmit power of S is set to $P_s = Q/|h_{SP}|^2$. Then, the SNR at R is equal to $\gamma_R = \bar{\gamma}_Q|h_{SR}|^2/|h_{SP}|^2$.

B. FSO Link

On the other hand, the behavior of the FSO link depends on three factors, which are path loss h_l, atmospheric turbulence h_a, and pointing error h_p. The path loss has a deterministic value, which is modeled by the exponential Beers–Lambert law, defined as [32]

$$h_l = \exp(-\sigma L), \tag{5}$$

where σ shows the atmospheric attenuation and L represents the distance between the relay and the destination node. Suppose that h_a is a RV that follows the DGG distribution, where its PDF is defined in [21], Eq. (7). Moreover, the PDF of h_p is given by [21], Eq. (9). The FSO channel gain is defined as $h_{RD} = h_l h_p h_a$ [32]. The electrical SNR at D is defined as $\gamma_D = (\eta h_{RD})^r/N_D$ [33]. Using [25], Eq. (9.31.2), the PDF of γ_D, which follows DGG distribution with consideration of pointing error and path loss, can be written as [4], Eq. (12). We have

$$f_{\gamma_D}(\gamma_D) = \frac{A_1}{\gamma_D} G^{m,0}_{\alpha_2 p,m}\left[B_1 g^{\alpha_2 p}\left(\frac{\gamma_D}{\mu_r}\right)^{\frac{\alpha_2 p}{r}}\middle|\begin{matrix}\kappa_1\\ \kappa_2\end{matrix}\right], \tag{6}$$

where $A_1 = \xi^2 p^{m_2-\frac{1}{2}} q^{m_1-\frac{1}{2}} (2\pi)^{1-\frac{r+q}{2}}/(r\Gamma(m_1)\Gamma(m_2))$, $B_1 = m_1^q m_2^p/(p^p q^q \Omega_1^q \Omega_2^p)$, $m = p+q+\alpha_2 p$, $\kappa_1 = [\bar{\Delta}(\alpha_2 p : \xi^2+1)]$, and $\kappa_2 = [\bar{\Delta}(\alpha_2 p : \xi^2), \bar{\Delta}(q : m_1), \bar{\Delta}(p : m_2)]$. The parameters of the turbulence channel (i.e., $\{\alpha_1, m_1, \Omega_1\}$ and $\{\alpha_2, m_2, \Omega_2\}$) are respectively described as both small- and large-scale atmospheric fluctuations, p and q are positive integer values such that $p/q = \alpha_1/\alpha_2$, and $g = A_1 B_1^{-1/(\alpha_2 p)} \prod_{i=1}^{p+q}(\alpha_2 p + \kappa_{0,i})/(\xi^2+1)$, where $\kappa_0 = [\Delta(q, m_1), \Delta(p, m_2)]$ while $\kappa_{l,i}$ represents the ith term of κ_l. Moreover, μ_r denotes the average electrical SNR of the FSO link for both types of detectors, which is defined as $\mu_r = (\eta \mathbb{E}[h_{RD}])^r/N_2$ and the value of this is obtained as $\mu_r = (h_l \eta A_0 g)^r/N_2$. ξ shows the ratio between the equivalent beam radius and the pointing error standard deviation at the receiver [32], which is given as $\xi = w_{z_{eq}}/(2\sigma_s)$, while $w_{z_{eq}}$ is the equivalent beam radius at the receiver and σ_s is the jitter variance at the receiver. Accordingly, the relationship between μ_r and $\bar{\gamma}_D$ is readily derived as

$$\bar{\gamma}_D = \begin{cases} \mu_1 & \text{if } r = 1, \\ (\sigma_{si}^2 + 1)\mu_2 & \text{if } r = 2, \end{cases} \tag{7}$$

where σ_{si}^2 is the scintillation index [32]. The CDF of γ_D can be written as [4], Eq. (14). We have

$$F_{\gamma_D}(\gamma_D) = A G^{rm,\alpha_2 p}_{(r+1)\alpha_2 p, rm+\alpha_2 p}\left[B\left(\frac{\gamma_D}{\mu_r}\right)^{\alpha_2 p}\middle|\begin{matrix}\kappa_3\\ \kappa_4\end{matrix}\right], \tag{8}$$

where $\kappa_3 = [\Delta(\alpha_2 p : 1), \kappa_A]$, $\kappa_4 = [\kappa_B, \Delta(\alpha_2 p : 0)]$, $\kappa_A = [\bar{\Delta}(r, \alpha_2 p, \xi^2+1)]$, and $\kappa_B = [\bar{\Delta}(r, \alpha_2 p, \xi^2), \bar{\Delta}(r, q, m_1), \bar{\Delta}(r, p, m_2)]$, while A and B are respectively defined as

$$A = \frac{\xi^2 p^{m_2-\frac{1}{2}} q^{m_1-\frac{1}{2}} (2\pi)^{1-\left(\frac{p+q}{2}\right)} r^{\mu-1}}{\Gamma(m_1)\Gamma(m_2)\alpha_2 p},$$
$$B = \left(\frac{g^{\alpha_2 p} m_1^q m_2^p}{p^p q^q \Omega_1^q \Omega_2^p r^{(p+q)}}\right)^r,$$

where $\mu = \sum_{j=1}^{\alpha_2 p} \kappa_{2,j} - \sum_{i=1}^{m} \kappa_{1,i} - \frac{p+q}{2} + 1$.

The overall SNR at the destination with the fixed gain dual-hop relaying can be written as

$$\gamma_F = \frac{\gamma_R \gamma_D}{\gamma_D + C}. \tag{9}$$

Using a semi-blind relay, $C = \bar{\gamma}_R + 1$ [8]. In the CSI-assisted relaying, the end-to-end SNR can be expressed as

$$\gamma_V = \frac{\gamma_R \gamma_D}{\gamma_R + \gamma_D + 1}. \tag{10}$$

III. Single Power Constraint Analysis

In this section, we consider a single power constraint strategy in an underlay CRN where the SU can use the PU's bandwidth simultaneously and in the same region, under the condition that interference power, which is imposed on the PU, should remain below the predefined value Q (known as IT) ([27], Eq. (4)).

A. Outage Probability

The OP is defined as the probability that the end-to-end SNR falls below a specified threshold, γ_{th}. It is given by

$$P_{\text{out}}(\gamma_{\text{th}}) = \Pr[\gamma_{e2e} \le \gamma_{\text{th}}] = F_{\gamma_{e2e}}(\gamma_{\text{th}}), \tag{11}$$

where $F_{\gamma_{e2e}}(\gamma_{\text{th}})$ denotes the CDF of γ_{e2e} evaluated at $\gamma = \gamma_{\text{th}}$. In the following, we derive the CDF of γ_{e2e} required to calculate Eq. (11).

1) Fixed Gain Relaying: Based on the law of probability, using the SNR distribution of the RF link and assuming Nakagami-m fading, the single power constraint strategy ([27], Eq. (22)), and finally employing Eqs. (8) and (9), the CDF of γ_F can be written as

$$\begin{aligned} F_{\gamma_F}(\gamma) &= \int_0^\infty F_{\gamma_R}\left(\frac{\gamma_D + C}{\gamma_D}\gamma\right) f_{\gamma_D}(\gamma_D) \mathrm{d}\gamma_D \\ &= 1 - \frac{a_{SP}^{m_{SP}}}{\Gamma(m_{SP})} \sum_{n=0}^{m_{SR}-1} \frac{\Gamma(m_{SP}+n)}{n!} \frac{(a_{SR}\gamma)^n \bar{\gamma}_Q^{m_{SP}}}{(a_{SP}\bar{\gamma}_Q + a_{SR}\gamma)^{m_{SP}+n}} I_1, \end{aligned} \tag{12}$$

where I_1 is defined by

$$\begin{aligned} I_1 = \int_0^\infty & \frac{A_1 \gamma_D^{m_{SP}-1} (\gamma_D + C)^n}{\left(\gamma_D + \frac{a_{SR} C \gamma}{a_{SP}\bar{\gamma}_Q + a_{SR}\gamma}\right)^{m_{SP}+n}} \\ & \times G^{m,0}_{\alpha_2 p,m}\left[B_1 g^{\alpha_2 p}\left(\frac{\gamma_D}{\mu_r}\right)^{\frac{\alpha_2 p}{r}}\middle|\begin{matrix}\kappa_1\\ \kappa_2\end{matrix}\right] \mathrm{d}\gamma_D. \end{aligned} \tag{13}$$

In order to solve I_1, we use the definition of binomial coefficients in [25], Eq. (1.111). Then by using [34], Eq. (2.24.2.4), and after some algebraic manipulations, the CDF of γ_F can be obtained as the top of the next page [Eq. (14)], where $\kappa_5 = [\Delta(\alpha_2 p : 1 - m_{SP} - k), \kappa_A]$ and $\kappa_6 = [\Delta(\alpha_2 p : n - k), \kappa_B]$. By applying $C = \mathbb{E}(\gamma_R) + 1$ to [27], Eq. (22), and utilizing [25], Eq. (3.326.2), $C = \bar{\gamma}_Q m_{SR} a_{SP}/((m_{SP}-1)a_{SR}) + 1$, which is only valid for $m_{SP} > 1$. As is clearly seen, there is a linear relation between C and $\bar{\gamma}_Q$ in the high-SNR regime.

- **Special case:**

As previously mentioned, Rayleigh and G^2 distributions are respectively special cases of Nakagami-m and DGG distributions. As a special case, it can be shown that for $m_{SR} = m_{SP} = 1$, $\alpha_1 = \alpha_2 = \Omega_1 = \Omega_2 = 1$, $m_1 = \alpha$, and $m_2 = \beta$ (i.e., Rayleigh/G^2 fading channels), the CDF in Eq. (14) simplifies to

$$F_{\gamma_F}(\gamma)=1-\frac{a_{SP}^{m_{SP}}}{\Gamma(m_{SP})}A(2\pi)^{1-\alpha_2 p}\sum_{n=0}^{m_{SR}-1}\sum_{k=0}^{n}\binom{n}{k}\frac{1}{n!}\frac{\bar{\gamma}_Q^{m_{SP}}(a_{SR}\gamma)^k(\alpha_2 p)^{m_{SP}+n}}{(a_{SR}\bar{\gamma}_Q+a_{SR}\gamma)^{m_{SP}+k}}G_{(r+1)\alpha_2 p,rm+\alpha_2 p}^{rm+\alpha_2 p,\alpha_2 p}\left[B\left(\frac{a_{SR}C\gamma}{\mu_r(a_{SP}\bar{\gamma}_Q+a_{SR}\gamma)}\right)^{\alpha_2 p}\middle|\begin{matrix}\kappa_5\\ \kappa_6\end{matrix}\right], \tag{14}$$

$$F_{\gamma_F}(\gamma)=1-\frac{A\bar{\gamma}_Q}{\bar{\gamma}_Q+\gamma}G_{r+1,3r+1}^{3r+1,1}\left[\frac{BC\gamma}{\mu_r(\bar{\gamma}_Q+\gamma)}\middle|\begin{matrix}0,\kappa_A\\ 0,\kappa_B\end{matrix}\right], \tag{15}$$

where A, B, g, κ_A, and κ_B in Eq. (14) are respectively reduced to $A=\xi^2 r^{\alpha+\beta-2}/(\Gamma(\alpha)\Gamma(\beta)(2\pi)^{(r-1)})$, $B=(g\alpha\beta/r^2)^r$, $g=\xi^2/(\xi^2+1)$, $\kappa_A=[(\xi^2+1)/r,\ldots,(\xi^2+r)/r]$, and $\kappa_B=[\xi^2/r,\ldots,(\xi^2+r-1)/r,\alpha/r,\ldots,(\alpha^2+r-1)/r,\beta/r,\ldots,(\beta^2+r-1)/r]$.

2) CSI-Assisted Relaying: It has been proved that the overall SNR of the CSI-assisted relaying can be tightly upper bounded by $\gamma_V^{\text{up}}=\min(\gamma_R,\gamma_D)$ [21]. Therefore, the CDF of γ_V^{up} is equal to

$$F_{\gamma_V^{\text{up}}}(\gamma)=1-F_{\gamma_R}^{\text{c}}(\gamma)F_{\gamma_D}^{\text{c}}(\gamma), \tag{16}$$

where $F_X^{\text{c}}(\gamma)=1-F_X(\gamma)$ is the complementary CDF of a RV X.

The OP of the CSI-assisted relaying system can be tightly lower bounded by $P_{\text{out}}^V(\gamma_{\text{th}})\geq F_{\gamma_V^{\text{up}}}(\gamma_{\text{th}})$. By substituting Eq. (8) and [27], Eq. (22), into Eq. (16), the CDF of γ_V^{up} can be derived as

$$F_{\gamma_V^{\text{up}}}(\gamma)=1+\frac{a_{SP}^{m_{SP}}}{\Gamma(m_{SP})}\sum_{k=0}^{m_{SR}-1}\frac{\Gamma(k+m_{SP})(a_{SR}\gamma)^k\bar{\gamma}_Q^{m_{SP}}}{k!(a_{SP}\bar{\gamma}_Q+a_{SR}\gamma)^{k+m_{SP}}}\times\left(AG_{(r+1)\alpha_2 p,rm+\alpha_2 p}^{rm,\alpha_2 p}\left[B\left(\frac{\gamma}{\mu_r}\right)^{\alpha_2 p}\middle|\begin{matrix}\kappa_3\\ \kappa_4\end{matrix}\right]-1\right). \tag{17}$$

Here, we can analyze extreme cases of Eqs. (14) and (17). It can be seen in Eqs. (14) and (17) that whenever $\bar{\gamma}_Q$ goes to zero, the PU cannot tolerate any additional interference. In this case, the OP is equal to $P_{\text{out}}(\gamma_{\text{th}})\approx 1$, which indicates that the SUs are not allowed to transmit anymore.

- **Special case:**

As another special case for Rayleigh/G^2 fading channels, it can be shown that the OP in [27], Eq. (22), reduces to $F_{\gamma_R}(\gamma)=\gamma/(\gamma+\bar{\gamma}_Q)$. Then, by substituting it and a simplified version of Eq. (8) for G^2 turbulence into Eq. (16), the CDF in Eq. (17) can be simplified as

$$F_{\gamma_V^{\text{up}}}(\gamma)=\frac{1}{\gamma+\bar{\gamma}_Q}\left(\gamma+\frac{A\bar{\gamma}_Q}{\gamma}G_{r,3r}^{3r,0}\left[B\frac{\gamma}{\mu_r}\middle|\begin{matrix}1,\kappa_A\\ \kappa_B,0\end{matrix}\right]\right). \tag{18}$$

B. Asymptotic Analysis

In order to provide insight about significant parameters that determine the network performance, we derive asymptotic expressions for the OP of fixed gain and CSI-assisted relaying in the high-SNR situation of the FSO and RF links. Without loss of generality, we assume $\bar{\gamma}\triangleq\bar{\gamma}_Q\triangleq d\mu_r$ ($\bar{\gamma}_Q$, $\mu_r\to\infty$), where d is a positive constant.

1) Fixed Gain Relaying: Similar to Eq. (12), by using [27], Eq. (21), Eq. (8), and the integral identity [34], Eq. (2.24.2.4), the CDF in Eq. (14) can be re-expressed as

$$F_{\gamma_F}(\gamma)=\sum_{n=0}^{\infty}\sum_{k=0}^{m_{SR}+n}\frac{\Theta_{n,k}a_{SP}^{m_{SP}+k}\gamma^k\bar{\gamma}^{m_{SP}}}{(a_{SP}\bar{\gamma}+a_{SR}\gamma)^{m_{SP}+k}}\times G_{(r+1)\alpha_2 p,rm+\alpha_2 p}^{rm+\alpha_2 p,\alpha_2 p}\left[B\left(\frac{a_{SR}dC\gamma}{\bar{\gamma}(a_{SP}\bar{\gamma}+a_{SR}\gamma)}\right)^{\alpha_2 p}\middle|\begin{matrix}\kappa_7\\ \kappa_8\end{matrix}\right], \tag{19}$$

where $\kappa_7\triangleq[\Delta(\alpha_2 p:1-m_{SP}-k),\kappa_A]$, $\kappa_8\triangleq[\Delta(\alpha_2 p:m_{SR}+n-k),\kappa_B]$, and $\Theta_{n,k}$ is given by

$$\Theta_{n,k}\triangleq\binom{m_{SR}+n}{k}\frac{Aa_{SR}^k(2\pi)^{1-\alpha_2 p}(\alpha_2 p)^{m_{SR}+m_{SP}+n}}{a_{SP}^k\Gamma(m_{SP})\Gamma(m_{SR}+n+1)}.$$

Although Eq. (19) is represented in terms of an infinite sum, it converges quickly to the exact result due to the gamma function in the denominator of expression $\Theta_{n,k}$. In the high-SNR situations of the network (i.e., $\bar{\gamma}\to\infty$), by using the Taylor series expansion of Meijer G-function in [25], Eq. (9.303), the CDF of the end-to-end SNR of fixed gain relaying in the asymptotic regime is obtained as

$$F_{\gamma_F}^{\infty}(\gamma)=\sum_{n=0}^{\infty}\sum_{k=0}^{m_{SR}+n}\sum_{i=1}^{rm+\alpha_2 p}\Theta_{n,k}\text{X}_{n,k,i}\left(\frac{\gamma}{\bar{\gamma}}\right)^{\alpha_2 p\kappa_{8,i}+k}, \tag{20}$$

where

$$\text{X}_{n,k,i}\triangleq\frac{\prod_{l=1,i\neq l}^{rm+\alpha_2 p}\Gamma(\kappa_{8,l}-\kappa_{8,i})\prod_{l=1}^{\alpha_2 p}\Gamma(1-\kappa_{7,l}+\kappa_{8,i})}{\prod_{l=\alpha_2 p+1}^{(r+1)\alpha_2 p}\Gamma(\kappa_{7,l}-\kappa_{8,i})}\times\left(B\left(\frac{dm_{SR}}{m_{SP}-1}\right)^{\alpha_2 p}\right)^{\kappa_{8,i}}.$$

Compared with Eq. (14) that is expressed in terms of the Meijer G-function, Eq. (20) includes only finite summations of elementary functions.

In the high-SNR regime, the OP can be represented as

$$P_{\text{out}}^{\infty}(\gamma_{\text{th}})=(G_c\bar{\gamma})^{-G_d}, \tag{21}$$

where G_d is the diversity order and G_c is the coding gain [35].

By keeping only the dominant terms of Eq. (20), G_d and G_c are given respectively by

$$G_d=\min\left\{m_{SR},\frac{\xi^2}{r},\frac{\alpha_1 m_1}{r},\frac{\alpha_2 m_2}{r}\right\}, \tag{22}$$

$$G_c = \frac{\lambda_X^{-1/G_d}}{\gamma_{\text{th}}}, \tag{23}$$

where for the fixed gain relaying with a single power constraint strategy (i.e., $\lambda_X = \lambda_A$) we have

$$\lambda_A \triangleq \begin{cases} \sum_{k=0}^{m_{SR}} \Theta_{0,k} \mathrm{X}_{0,k,1} & \text{if } G_d = \mathrm{m}_{SR}, \\ \sum_{n=0}^{\infty} \Theta_{n,0} \mathrm{X}_{n,0,u_1} & \text{if } G_d = \frac{\xi^2}{r}, \\ \sum_{n=0}^{\infty} \Theta_{n,0} \mathrm{X}_{n,0,u_2} & \text{if } G_d = \frac{\alpha_1 m_1}{r}, \\ \sum_{n=0}^{\infty} \Theta_{n,0} \mathrm{X}_{n,0,u_3} & \text{if } G_d = \frac{\alpha_2 m_2}{r}, \end{cases} \tag{24}$$

while $u_1 = (r+1)\alpha_2 p - r + 1$, $u_2 = (r+1)\alpha_2 p + r(q-1) + 1$, and $u_3 = r(m-1) + \alpha_2 p + 1$. This indicates that the diversity order in Eq. (22) is a function of the $S \to R$ severity parameter (i.e., m_{SR}), FSO turbulence parameters (i.e., α_1, m_1, α_2, and m_2), pointing error (i.e., ξ), and the detection method in the destination (i.e., r). However, unlike the coding gain given in Eq. (23), its value is independent of PN parameters.

2) CSI-Assisted Relaying: Similarly, in the high-SNR situations of the CSI-assisted scenario, by assuming $F_{\gamma_R}^{\infty}(\gamma) F_{\gamma_D}^{\infty}(\gamma) \overset{\bar{\gamma}\to\infty}{\ll} F_{\gamma_R}^{\infty}(\gamma) + F_{\gamma_D}^{\infty}(\gamma)$, using [25], Eq. (9.303), and [27], Eq. (28), and keeping only the dominant terms, Eq. (17) is reduced to

$$F_{\gamma_V^{\text{up}}}^{\infty}(\gamma) = \sum_{i=1}^{rm} \mathrm{Z}_i \left(\frac{\gamma}{\bar{\gamma}}\right)^{\alpha_2 p \kappa_{4,i}} + \varphi \left(\frac{\gamma}{\bar{\gamma}}\right)^{m_{SR}}, \tag{25}$$

where

$$\mathrm{Z}_i \triangleq \frac{A \prod_{l=1, i\neq l}^{rm} \Gamma(\kappa_{4,l} - \kappa_{4,i}) \prod_{l=1}^{\alpha_2 p} \Gamma(1 - \kappa_{3,l} + \kappa_{4,i})}{\prod_{l=\alpha_2 p+1}^{(r+1)\alpha_2 p} \Gamma(\kappa_{3,l} - \kappa_{4,i}) \prod_{l=rm+1}^{rm+\alpha_2 p} \Gamma(1 - \kappa_{4,l} + \kappa_{4,i})} (dB)^{\kappa_{4,i}},$$

$$\varphi \triangleq \frac{\Gamma(m_{SR} + m_{SP})}{\Gamma(m_{SR}+1)\Gamma(m_{SP})} \left(\frac{a_{SR}}{a_{SP}}\right)^{m_{SR}}.$$

Having Eqs. (21) and (25) in our hand, the diversity order and coding gain of this scenario are respectively the same as those in Eqs. (22) and (23), where for the CSI-assisted relaying with a single power constraint strategy (i.e., $\lambda_X = \lambda_B$), λ_B becomes

$$\lambda_B \triangleq \begin{cases} \varphi & \text{if } G_d = m_{SR}, \\ \mathrm{Z}_{v_1} & \text{if } G_d = \frac{\xi^2}{r}, \\ \mathrm{Z}_{v_2} & \text{if } G_d = \frac{\alpha_1 m_1}{r}, \\ \mathrm{Z}_{v_3} & \text{if } G_d = \frac{\alpha_2 m_2}{r}, \end{cases} \tag{26}$$

while $v_1 = r(\alpha_2 p - 1) + 1$, $v_2 = r\alpha_2 p + r(q-1) + 1$, and $v_3 = r(m-1) + 1$.

IV. Two Power Constraints Analysis

In order to consider a more realistic assumption, we consider that the transmitted power of the SU is restricted due to hardware limitations. In this section, we suppose that in addition to the IT constraint, which is imposed by underlay CRN, the SU's power is limited to a constant power. Therefore, there are two power constraints [i.e., the IT constraint (Q) and the maximum transmit power constraint ($P_{\max}$)].

A. Outage Probability

1) Fixed Gain Relaying: Using the same approach as in the previous section, we can derive the CDF of a fixed gain relaying system with both power constraints. Therefore, by using Eq. (8), Eq. (9), and the CDF of the RF link SNR in the presence of IT and the maximum transmit power constraint as in [27], Eq. (12), the CDF of γ_F can be written as

$$F_{\gamma_F}(\gamma) = 1 - \frac{\Upsilon\left(m_{SP}, a_{SP}\frac{\bar{\gamma}_Q}{\bar{\gamma}_P}\right)}{\Gamma(m_{SP})}(I_2 + 1) - \frac{A_1 a_{SP}^{m_{SP}}}{\Gamma(m_{SP})} I_3, \tag{27}$$

where, as detailed in Appendix A, I_2 and I_3 are given respectively at the top of the next page. $D_1 \triangleq (a_{SP}\bar{\gamma}_Q + a_{SR}\gamma)\mu_r / (B_1^{r/(\alpha_2 p)} g^r C a_{SR})$, $D_2 \triangleq \bar{\gamma}_P \mu_r / (B_1^{r/(\alpha_2 p)} g^r C a_{SR})$, and κ_9 and κ_{10} are given respectively by

$$\kappa_9 = 1 - \kappa_2 - (m_{SP} + i - k)\left[\frac{r}{\alpha_2 p}\right]_m ; \left[\frac{r}{\alpha_2 p}\right]_m, \left[\frac{r}{\alpha_2 p}\right]_m,$$

$$\kappa_{10} = 1 - \kappa_1 - (m_{SP} + i - k)\left[\frac{r}{\alpha_2 p}\right]_{\alpha_2 p} ; \left[\frac{r}{\alpha_2 p}\right]_{\alpha_2 p}, \left[\frac{r}{\alpha_2 p}\right]_{\alpha_2 p}.$$

Note that the EGBFHF is efficiently implemented in Mathematica in Ref. [36]. We have

$$I_2 = 1 - A(2\pi)^{-\frac{1}{2}(\alpha_2 p - 1)} e^{-a_{SR}\frac{\gamma}{\bar{\gamma}_P}} \sum_{m=0}^{m_{SR}-1} \sum_{k=0}^{m} \binom{m}{k} \frac{(\alpha_2 p)^{m-k+\frac{1}{2}}}{m!} \left(\frac{a_{SR}}{\bar{\gamma}_P}\gamma\right)^k \times G_{r\alpha_2 p, rm+\alpha_2 p}^{rm+\alpha_2 p, 0}\left[B\left(\frac{a_{SR} C}{\alpha_2 p}\frac{\gamma}{\bar{\gamma}_P \mu_r}\right)^{\alpha_2 p} \middle| \begin{matrix} \kappa_A \\ \kappa_B, \Delta(\alpha_2 p : m-k) \end{matrix} \right], \tag{28}$$

$$I_3 = \exp\left(-\frac{a_{SR}\gamma + a_{SP}\bar{\gamma}_Q}{\bar{\gamma}_P}\right) \sum_{n=0}^{m_{SR}-1} \sum_{k=0}^{m_{SP}+n-1} \sum_{i=0}^{n} \binom{n}{i} \left(\frac{a_{SR} C}{\bar{\gamma}_Q}\gamma\right)^{k-m_{SP}} \frac{\Gamma(m_{SP}+n) C^{-i}}{n! k! \Gamma(m_{SP}+n-m)\alpha_2 p} \times \left(\frac{\bar{\gamma}_Q}{\bar{\gamma}_P}\right)^k \left(B_1^{r/(\alpha_2 p)} g^r \left(\frac{1}{\mu_r}\right)\right)^{k-i-m_{SP}} H_{m,\alpha_2 p : 1,0 : 1,1}^{m,0:0,1:1,1}\left[\begin{matrix} \kappa_9 \\ \kappa_{10} \end{matrix} \middle| \begin{matrix} (k-n-m_{SP}+1, 1) \\ (0,1) \end{matrix} \middle| \begin{matrix} (1,1) \\ - \end{matrix} \middle| D_1/\gamma, D_2/\gamma \right]. \tag{29}$$

By applying $C = \mathbb{E}(\gamma_R) + 1$ to [27], Eq. (12), and using [25], Eqs. (3.351.1) and (3.351.2), the C parameter of semi-blind fixed gain relaying with two power constraints is calculated as

$$C = \frac{a_{SP} m_{SR}}{a_{SR}\Gamma(m_{SP})}\left(\bar{\gamma}_Q \Gamma\left(m_{SP}-1, \frac{\bar{\gamma}_Q}{\bar{\gamma}_P}\right) + \frac{\bar{\gamma}_P}{a_{SP}} \Upsilon\left(m_{SP}, \frac{\bar{\gamma}_Q}{\bar{\gamma}_P}\right)\right) + 1. \tag{30}$$

As can be seen in Eq. (30), by increasing the power limitation quantities of the RF link (i.e., $\bar{\gamma}_Q$ and $\bar{\gamma}_P$) at the same time, the value of C increases linearly.

- **Special case:**

It can be shown that for $m_{SR} = m_{SP} = 1$ (i.e., Rayleigh fading) and $\alpha_1 = \alpha_2 = \Omega_1 = \Omega_2 = 1$, $m_1 = \alpha$, $m_2 = \beta$ (i.e., G^2 fading), the OP in Eq. (27) simplifies to

$$\begin{aligned} F_{\gamma_F}(\gamma) = {} & 1 - A\left(1 - e^{-\frac{\bar{\gamma}_Q}{\bar{\gamma}_P}}\right) G^{3r+1,0}_{r,3r+1}\left[\frac{B\gamma C}{\bar{\gamma}_P \mu_r}\middle| \begin{matrix}\kappa_A \\ \kappa_B, 0\end{matrix}\right] \times e^{-a_{SR}\frac{\gamma}{\bar{\gamma}_P}} \\ & + \frac{A(2\pi)^{r-1}}{B r^{\alpha+\beta+2r-2}} \exp\left(-\frac{\gamma+\bar{\gamma}_Q}{\bar{\gamma}_P}\right)\left(\frac{\bar{\gamma}_Q \mu_r}{C\gamma}\right) \\ & \times H^{3,0:0,1:1,1}_{3,1:1,0:1,1}\left[\begin{matrix}\kappa_{11} \\ \kappa_{12}\end{matrix}\middle| \begin{matrix}(0,1) \\ (0,1)\end{matrix}\middle| \begin{matrix}(1,1) \\ -\end{matrix}\middle| D_3/\gamma, D_4/\gamma\right], \end{aligned} \tag{31}$$

where $\kappa_{11} \triangleq [(1-\xi^2-r, r; r), (1-\alpha-r, r; r), (1-\beta-r, r; r)]$, $\kappa_{12} \triangleq [-\xi^2 - r, r; r]$, $D_3 \triangleq (\gamma + \bar{\gamma}_Q)\mu_r/(C(g\alpha\beta)^r)$, and $D_4 \triangleq \bar{\gamma}_P \mu_r/(C(g\alpha\beta)^r)$. The simplified versions of A, B, g, κ_A, and κ_B are defined in the special case of Section III after Eq. (15). Note that an expression with the same value as Eq. (31) was previously reported in [17], Eq. (7). However, Eq. (31) is more efficient than [17], Eq. (7), since it just needs evaluation of one EGBFHF, while the expression in [17], Eq. (7), has two EGBFHFs.

2) CSI-Assisted Relaying: The upper-bounded CDF of the overall SNR of the CSI-assisted relaying is derived by substituting Eq. (8) and [27], Eq. (12), into Eq. (16) as follows:

$$\begin{aligned} F^{\text{up}}_{\gamma_V}(\gamma) = {} & \left(\frac{\Upsilon(m_{SR}, a_{SR}\gamma/\bar{\gamma}_P)}{\Gamma(m_{SR})}\frac{\Upsilon(m_{SP}, a_{SP}\bar{\gamma}_Q/\bar{\gamma}_P)}{\Gamma(m_{SP})}\right. \\ & - \sum_{n=0}^{m_{SR}-1} \frac{(a_{SR}\gamma)^n a_{SP}^{m_{SP}} \bar{\gamma}_Q^{m_{SP}}}{n!\Gamma(m_{SP})(a_{SP}\bar{\gamma}_Q + a_{SR}\gamma)^{m_{SP}+n}} \\ & \left.\times \Gamma\left(m_{SP}+n, \frac{a_{SP}\bar{\gamma}_Q + a_{SR}\gamma}{\bar{\gamma}_P}\right)\right) \\ & \times \left(1 - A G^{rm,\alpha_2 p}_{(r+1)\alpha_2 p, rm+\alpha_2 p}\left[B\left(\frac{\gamma}{\mu_r}\right)^{\alpha_2 p}\middle| \begin{matrix}\kappa_3 \\ \kappa_4\end{matrix}\right]\right) \\ & + A G^{rm,\alpha_2 p}_{(r+1)\alpha_2 p, rm+\alpha_2 p}\left[B\left(\frac{\gamma}{\mu_r}\right)^{\alpha_2 p}\middle| \begin{matrix}\kappa_3 \\ \kappa_4\end{matrix}\right] \\ & + \frac{\Gamma(m_{SP}, a_{SP}\bar{\gamma}_Q/\bar{\gamma}_P)}{\Gamma(m_{SP})}. \end{aligned} \tag{32}$$

- **Special case:**

For $m_{SR} = m_{SP} = 1$ and $\alpha_1 = \alpha_2 = \Omega_1 = \Omega_2 = 1$, the CDF in Eq. (32) reduces to [16], Eq. (7), which was obtained for Rayleigh/G^2 fading channels.

B. Asymptotic Analysis

Similar to Subsection III.B, we focus on asymptotic results for fixed gain and CSI-assisted relaying to derive diversity gains. Without loss of generality, we assume that $\bar{\gamma} \triangleq \bar{\gamma}_Q \triangleq d_1\bar{\gamma}_P \triangleq d_2\mu_r$ ($\bar{\gamma}_Q$, $\bar{\gamma}_P$, $\mu_r \to \infty$), where d_1 and d_2 are arbitrary positive constants.

1) Fixed Gain Relaying: The lower and upper incomplete gamma functions in [27], Eq. (11), can be expanded in terms of a Taylor series by using [25], Eqs. (8.352.1) and (8.352.2), respectively. We have

$$\begin{aligned} F_{\gamma_F}(\gamma) = {} & \sum_{n=0}^{\infty}\sum_{k=0}^{m_{SR}+n} \frac{\Theta_{n,k} a_{SP}^{m_{SP}+k}\gamma^k \bar{\gamma}^{m_{SP}}}{(a_{SP}\bar{\gamma} + a_{SR}\gamma)^{m_{SP}+k}} G^{rm+\alpha_2 p, \alpha_2 p}_{(r+1)\alpha_2 p, rm+\alpha_2 p}\left[B\left(\frac{a_{SR}C\gamma}{\bar{\gamma}(a_{SP}\bar{\gamma} + a_{SR}\gamma)}\right)^{\alpha_2 p}\middle| \begin{matrix}\kappa_7 \\ \kappa_8\end{matrix}\right] \\ & - \sum_{n=0}^{\infty}\sum_{i=0}^{\infty}\sum_{j=0}^{n}\sum_{k=0}^{m_{SR}+i} \Xi_{n,i,j,k}\Lambda_{n,i,j,k}\left(1 + \frac{a_{SR}\gamma}{a_{SP}\bar{\gamma}}\right)^j \left(\frac{C a_{SR}\Gamma(m_{SP})}{\bar{\gamma} m_{SR}\theta}\right)^{m_{SR}+n+i-k-j}\left(\frac{\gamma}{\bar{\gamma}}\right)^{m_{SR}+n+i-j} \\ & + \sum_{n=0}^{\infty}\sum_{k=0}^{m_{SR}+n} \Psi_{n,k}\Phi_{n,k}\left(\frac{C a_{SR}\Gamma(m_{SP})}{\bar{\gamma} m_{SR}\theta}\right)^{m_{SR}+n-k}\left(\frac{\gamma}{\bar{\gamma}}\right)^{m_{SR}+n}. \end{aligned} \tag{33}$$

$$\begin{aligned} \Lambda_{n,i,j,k} & \triangleq \binom{n}{j}\binom{m_{SR}+i}{k}\frac{(-1)^n A_1 a_{SP}^{m_{SP}+j} a_{SR}^k d_1^{m_{SR}+m_{SP}+n+i}}{n!(m_{SR}+m_{SP}+n+i)\Gamma(m_{SR}+i+1)\Gamma(m_{SP})}, \\ \Xi_{n,i,j,k} & \triangleq \frac{\prod_{l=1}^{m}\Gamma\left(-\frac{r}{\alpha_2 p}(m_{SR}+n+i-k-j)+\kappa_{2,l}\right)}{\prod_{l=1}^{\alpha_2 p}\Gamma\left(-\frac{r}{\alpha_2 p}(m_{SR}+n+i-k-j)+\kappa_{1,l}\right)}\left(\frac{d_2 m_{SR}\theta}{\Gamma(m_{SP})} g^r B_1^{\frac{r}{\alpha_2 p}}\right)^{m_{SR}+n+i-k-j}, \\ \Phi_{n,k} & \triangleq \binom{m_{SR}+n}{k}\frac{(-1)^n A_1 a_{SR}^k \Upsilon(m_{SP}, a_{SP}d_1)}{n!(m_{SR}+n)\Gamma(m_{SR})\Gamma(m_{SP})}, \\ \Psi_{n,k} & \triangleq \frac{\prod_{l=1}^{m}\Gamma\left(-\frac{r}{\alpha_2 p}(m_{SR}+n-k)+\kappa_{2,l}\right)}{\prod_{l=1}^{\alpha_2 p}\Gamma\left(-\frac{r}{\alpha_2 p}(m_{SR}+n-k)+\kappa_{1,l}\right)}\left(\frac{d_2 m_{SR}\theta}{\Gamma(m_{SP})} g^r B_1^{\frac{r}{\alpha_2 p}}\right)^{m_{SR}+n-k}. \end{aligned} \tag{34}$$

By using the resulting expressions, Eq. (8) and the integral identities in [34], Eqs. (2.24.2.1) and (2.24.2.4), the end-to-end CDF of fixed gain relaying SNR is obtained as in Eq. (33), where $\theta \triangleq a_{SP}\Gamma(m_{SP}-1,d_1)+\Upsilon(m_{SP},d_1)$, while $\Lambda_{n,i,j,k}$, $\Xi_{n,i,j,k}$, $\Phi_{n,k}$, and $\Psi_{n,k}$ are defined in Eq. (34). At high SNRs, Eq. (30) simplifies to $C=\bar{\gamma}m_{SR}\theta/(a_{SR}\Gamma(m_{SP}))+1$. In the high-SNR regime, by keeping only the dominant terms, Eq. (33) reduces to

$$F_{\gamma_F}^{\infty}(\gamma)=\sum_{n=0}^{\infty}\sum_{k=0}^{m_{SR}+n}\sum_{i=1}^{rm+\alpha_2 p}\Theta_{n,k}\Upsilon_{n,k,i}\left(\frac{\gamma}{\bar{\gamma}}\right)^{\alpha_2 p\kappa_{8,i}+k}-\sum_{n=0}^{\infty}\sum_{i=0}^{\infty}\sum_{j=0}^{n}\sum_{k=0}^{m_{SR}+i}\Lambda_{n,i,j,k}\Xi_{n,i,j,k}\left(\frac{\gamma}{\bar{\gamma}}\right)^{m_{SR}+n+i-j}+\sum_{n=0}^{\infty}\sum_{k=0}^{m_{SR}+n}\Phi_{n,k}\Psi_{n,k}\left(\frac{\gamma}{\bar{\gamma}}\right)^{m_{SR}+n},\tag{35}$$

where

$$\Upsilon_{n,k,i}\triangleq\frac{\prod_{l=1,i\neq l}^{rm+\alpha_2 p}\Gamma(\kappa_{8,l}-\kappa_{8,i})\prod_{l=1}^{\alpha_2 p}\Gamma(1-\kappa_{7,l}+\kappa_{8,i})}{\prod_{l=\alpha_2 p+1}^{(r+1)\alpha_2 p}\Gamma(\kappa_{7,l}-\kappa_{8,i})}\times\left(B\left(\frac{d_2\theta m_{SR}}{a_{SP}\Gamma(m_{SR})}\right)^{\alpha_2 p}\right)^{\kappa_{8,i}}.\tag{36}$$

In comparison to Eq. (27), which is expressed in terms of Meijer G and bivariate Fox H-functions, Eq. (35) includes only finite summations of the elementary function.

Again, the asymptotic OP can be expressed as in Eq. (21), where the diversity order and coding gain are respectively given in Eqs. (22) and (23), while $\lambda_X=\lambda_C$ and

$$\lambda_C\triangleq\begin{cases}\sum_{k=0}^{m_{SR}}\Theta_{0,k}\Upsilon_{0,k,1}+\Lambda_{0,0,0,k}\Xi_{0,0,0,k}+\Phi_{0,k}\Psi_{0,k} & \text{if } G_d=m_{SR},\\ \sum_{n=0}^{\infty}\Theta_{n,0}\Upsilon_{n,0,u_1} & \text{if } G_d=\frac{\xi^2}{r},\\ \sum_{n=0}^{\infty}\Theta_{n,0}\Upsilon_{n,0,u_2} & \text{if } G_d=\frac{\alpha_1 m_1}{r},\\ \sum_{n=0}^{\infty}\Theta_{n,0}\Upsilon_{n,0,u_3} & \text{if } G_d=\frac{\alpha_2 m_2}{r}.\end{cases}\tag{37}$$

This indicates that the diversity order for the two power constraints strategy is the same as the single power constraint ones. However, the coding gains are different.

2) CSI-Assisted Relaying: For the CSI-assisted scenario, using [25], Eq. (9.303), and [27], Eq. (16), the asymptotic expression of Eq. (32) is derived as

$$F_{\gamma_V^{\text{up}}}^{\infty}(\gamma)=\sum_{i=1}^{rm}\mathrm{Z}_i\left(\frac{\gamma}{\bar{\gamma}}\right)^{\alpha_2 p\kappa_{4,i}}+\phi\left(\frac{\gamma}{\bar{\gamma}}\right)^{m_{SR}},\tag{38}$$

where

$$\phi\triangleq\left[\frac{\Upsilon(m_{SP},d_1 a_{SP})a_{SR}^{m_{SR}}}{\Gamma(m_{SR}+1)\Gamma(m_{SP})}+\frac{\Gamma(m_{SR}+m_{SP},d_1 a_{SP})}{\Gamma(m_{SR}+1)\Gamma(m_{SP})}\left(\frac{a_{SR}}{d_1 a_{SP}}\right)^{m_{SR}}\right].\tag{39}$$

Similar to Eq. (26), the asymptotic OP, diversity order, and coding gain are given by Eqs. (21), (22), and (23), respectively, where $\lambda_X=\lambda_D$ and λ_D is defined as

$$\lambda_D\triangleq\begin{cases}\phi & \text{if } G_d=m_{SR},\\ \mathrm{Z}_{v_1} & \text{if } G_d=\frac{\xi^2}{r},\\ \mathrm{Z}_{v_2} & \text{if } G_d=\frac{\alpha_1 m_1}{r},\\ \mathrm{Z}_{v_3} & \text{if } G_d=\frac{\alpha_2 m_2}{r}.\end{cases}\tag{40}$$

Again, the diversity order of the two power constraints strategy is the same as the aforementioned single power constraint in Subsection III.B. Also, the diversity order of SN is independent of PN link parameters. These phenomena show that the maximum transmit power constraint and IT are just impressed by the coding gain.

V. Comparison Between Two Scenarios

A. Diversity and Coding Gain

With comparison between the asymptotic expressions of the OP for the single and two power constraint strategies for both fixed gain and CSI-assisted relaying techniques, they have the same diversity order, where its value is independent of interference link parameters and it is just limited by the RF-FSO links' parameters. However, there is a gap between the single and two power constraints strategies, defined as G_1 and G_2 for fixed gain and CSI-assisted techniques, respectively. These quantities are defined respectively as

$$G_1=10\log_{10}\left(\frac{\lambda_C}{\lambda_A}\right)^{\frac{1}{G_d}},\qquad G_2=10\log_{10}\left(\frac{\lambda_D}{\lambda_B}\right)^{\frac{1}{G_d}}.\tag{41}$$

B. Diversity-Multiplexing Trade-Off

The threshold SNR (i.e., γ_{th}) is a function of spectral efficiency R as $\gamma_{\text{th}}=2^{2R}-1$ (for half-duplex relaying). The spectral efficiency can be denoted by channel capacity R and normalized spectral efficiency t as $R=t\log_2(1+\bar{\gamma})$. Therefore, the diversity-multiplexing trade-off can be formulated as [35]

$$d(t)=\lim_{\bar{\gamma}\to\infty}\frac{-\log P_{\text{out}}(\bar{\gamma},t)}{\log\bar{\gamma}}.\tag{42}$$

Using Eqs. (42) and (22), the diversity-multiplexing trade-off can be written as

$$d(t)=\min\left(m_{SR},\frac{\xi^2}{r},\frac{\alpha_1 m_1}{r},\frac{\alpha_2 m_2}{r}\right)(1-2t).\tag{43}$$

The maximum diversity gain, when $(t\to 0)$, is achieved as $\min(m_{SR},\xi^2/r,\alpha_1 m_1/r,\alpha_2 m_2/r)$ and the maximum normalized spectral efficiency, when $(d\to 0)$, is equal to $t=1/2$.

VI. Numerical Results

In order to verify our analytical results, we now compare the derived expressions against Monte Carlo simulations. We suppose a two-dimensional plane ($[x, y]$) for the location of all nodes. We have assumed that the channel mean power of each link is proportional to the inverse of the fourth power of their distance i.e., $\Omega_{UV} = d_{UV}^{-4}$, where d_{UV} is the distance between the U and V nodes. We assume that the SUs are located on the x axis; i.e., the S, R, and D locations are [0, 0], [1/2, 0], and [1, 0], respectively, and the location of the PU is [0.5, 0.5]; hence, $\Omega_{SR} = 16$ and $\Omega_{SP} = 4$ (a unit in this plane is a kilometer). The attenuation coefficient of the FSO link is equal to $\sigma = 0.43$ dB/km, which is considered for the clear air condition [9]. For the FSO link, the following parameters for strong and moderate turbulence conditions are respectively assumed:

- $m_1 = 0.5$, $m_2 = 1.8$, $\Omega_1 = 1.5074$, $\Omega_2 = 0.928$, $\alpha_1 = 1.8621$, $\alpha_2 = 1$,
- $m_1 = 0.55$, $m_2 = 2.35$, $\Omega_1 = 1.5793$, $\Omega_2 = 0.9671$, $\alpha_1 = 2.169$, $\alpha_2 = 1$.

Figure 2 shows the OP performance of the mixed RF-FSO system, assuming the two power constraints strategy. The analytical expression is based on Eq. (27), which corresponds to the exact expression for fixed gain relaying. The OP is illustrated with respect to the average SNR of the RF link for a given fixed average electrical SNR of the FSO link. We assume strong turbulence conditions and direct detection IM/DD with $m_{SP} = 3$ and $\xi = 7.35$. As expected, by increasing $P_{\max}$, m_{SR}, or $\bar{\gamma}_D$, the outage performance improves. As observed, by increasing $\bar{\gamma}_Q$, the OP decreases. The behavior of the OP can be categorized into two regions. Before 15 dB, the OP decreases with increasing SNR. After 15 dB, it results in an error floor, as expected from our high-SNR analysis. This phenomena is due to the aforementioned maximum power limitation of the SU (i.e., $P_{\max}$).

Figure 3 demonstrates the OP performance of the mixed RF-FSO system, assuming both power constraint strategies. Strong turbulence conditions and direct detection

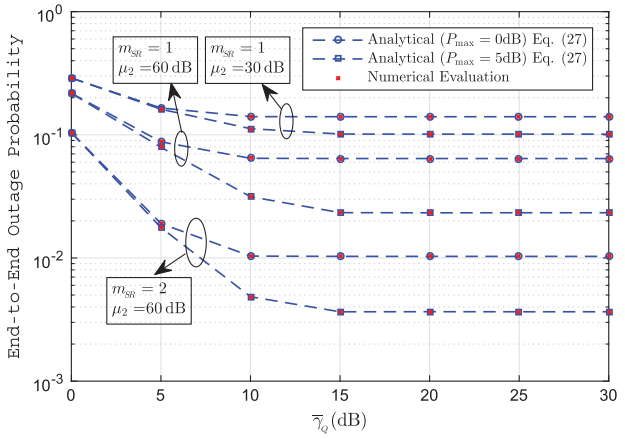

Fig. 2. Outage probability of the fixed gain relaying system under strong turbulence conditions with the IM/DD technique.

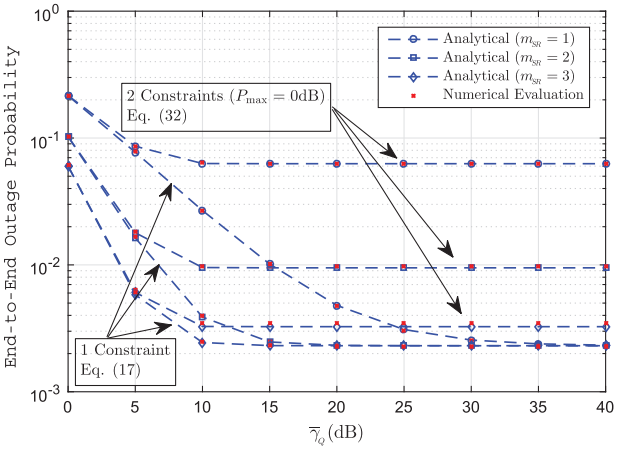

Fig. 3. Outage probability versus average power of the RF link for CSI-assisted relaying under strong turbulence conditions with the IM/DD technique.

are assumed. The other parameters are listed as $\mu_r = 60$ dB, $\xi = 7.35$, $m_{SP} = 3$, and $P_{\max} = 0$ dB. The analytical results for the OP of CSI-assisted relaying are based on the derived expressions in Eqs. (17) and (32), which are obtained for single power constraint and two power constraints strategies, respectively. As can be seen for both strategies, by increasing μ_r, the OP decreases. However, after a certain point, an error floor takes place. For the first strategy, it comes from the fact that if the SNR of one link grows with no bound as in Eq. (10), the other link's SNR becomes dominant. Therefore, since $\mu_r = 60$ dB, the FSO link's SNR is dominated and an error floor occurs. However, for the second one, $P_{\max}$ is the reason for saturation. As expected, by increasing m_{SR}, the performance improves. It is observed that the first strategy achieves lower outage than the second one, as expected. For example, in the case of $m_{SR} = 2$, to achieve an OP of 10^{-2}, a SNR of 15 dB is required for the two power constraints strategy, while this decreases to 7 dB in the case of the single power constraint strategy. This performance improvement comes at the cost of a less practical system.

Figure 4 presents the OP of the mixed RF-FSO system with respect to the average SNR of the FSO link for both CSI-assisted and fixed gain relaying scenarios, assuming a single power constraint strategy. It is observed that the simulation results of fixed gain relaying are in excellent agreement with the derived expression in Eq. (14), indicating its accuracy. Also, the proposed analytical lower bound for CSI-assisted relaying in Eq. (17) yields excellent tightness across the entire SNR range and becomes exact at high SNRs. As expected, for the moderate atmospheric turbulence, the performance gets better. Specifically for CSI-assisted relaying, to achieve an OP $= 10^{-2}$, a SNR of 50 dB is required for strong turbulence conditions, while this decreases to 40 dB for moderate conditions. It is observed that the CSI-assisted relaying has better performance than the fixed gain relaying system.

Figure 5 illustrates the analytical expression for the OP of fixed gain relaying, assuming the single power constraint

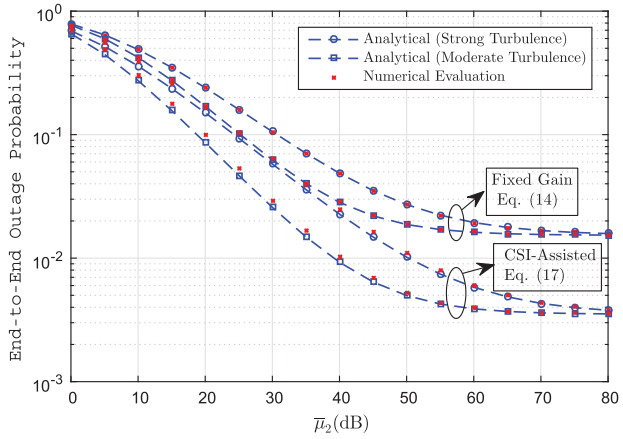

Fig. 4. Outage probability versus average power of the FSO link with the single power constraint strategy.

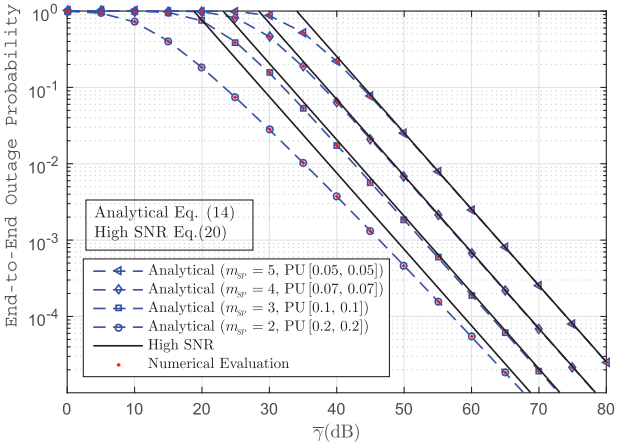

Fig. 6. Outage probability versus $\bar{\gamma}$ under moderate turbulence conditions for fixed gain relaying with the IM/DD technique.

strategy in Eq. (14) against the global average SNR (i.e., $\bar{\gamma}$). Contrary to the previous figures, saturation does not occur in Fig. 5 since the SNRs of both links increase simultaneously. The fading channel parameter m_{SP} is taken as equal to 2. It is observed that the heterodyne system achieves lower outage than the IM/DD method, as expected. For example, in the case of perfect alignment and assuming $m_{SR} = 2$, to achieve an OP of 10^{-4}, a 40 dB SNR is required for the heterodyne detection method, while this increases to 75 dB in the case of the IM/DD method. This performance improvement comes at the cost of a more complex receiver. It can also be observed that performance improves as the effect of the pointing error decreases. For example, for the heterodyne detection method, to achieve OP $= 10^{-4}$, 40 dB is required for the perfect alignment case, while this increases to 50 dB in the case of pointing error. The high-SNR expression in Eq. (20) can very efficiently predict the exact OP. Here, only the dominant term of Eq. (20) is considered, which yields excellent tightness across the moderate and high-SNR ranges. The diversity orders from lowest toward highest outage curves are equal to 1.19, 1.104, 1, 0.6, and 0.47, which also confirm our derived expression in Eq. (22).

Figure 6 demonstrates the OP as a function of $\bar{\gamma}$ for various locations of the PU. The single power constraint strategy and fixed gain relaying are employed. As expected, by decreasing the distance between the secondary source and the PU, the performance degrades. As can be seen, in Eq. (20) different values of m_{SP} and locations of the PU led to distinct values of $\Theta_{n,k}$. Consequently, the obtained coding gains are not equal. However, the diversity orders that confirm the derived expressions in Eqs. (22) and (23) are the same. As observed, the simulation results confirm our analytical derivations in Eqs. (14) and (20).

Finally, in order to show distinction between the single and two power constraint strategies, Fig. 7 presents the SNR gain of the first strategy with respect to the second one as a function of Euclidean distance between the PU and S for the fixed gain relaying network. The analytical

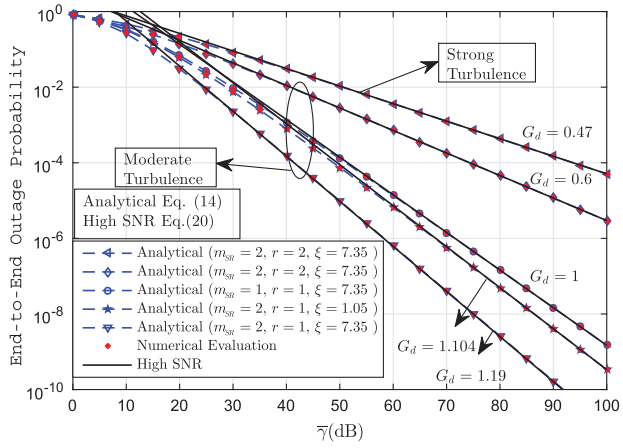

Fig. 5. Outage probability of fixed gain relaying versus the global average SNR ($\bar{\gamma}$).

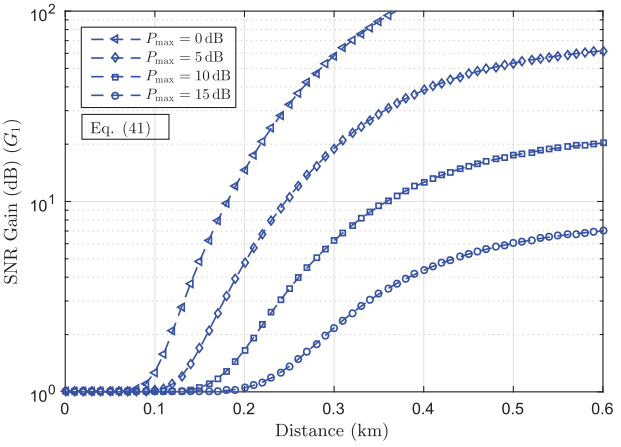

Fig. 7. SNR gap between single and two power constraints strategies versus the distance between the PU and S under moderate turbulence conditions for fixed gain relaying with the heterodyne detection technique.

expression is based on the first equation of Eqs. (41). The SNR and fading severity of the RF link are set to $\gamma_R = 20$ dB and $m_{SR} = 2$, respectively, and $m_{SP} = 2$ is considered for the interference link. We consider strong turbulence conditions and heterodyne detection with $\mu_r = 60$ dB for the FSO link. As observed, when the distance is small there is no SNR gain. However, by increasing the distance, the SNR gain increases, too. As expected, by increasing $P_{\max}$ the SNR gain decreases. This can be explained as follows. When the PU is close to S, h_{SP} becomes strong. Therefore, the source power for both strategies is limited by the constraint $Q/|h_{SP}|^2$. However, when the PU is far from S, h_{SP} becomes weak and the power of S is limited only by the maximum transmit power of the SU and the power limitation based on the IT constraint can be neglected.

VII. Conclusion

We assessed the performance of a mixed RF-FSO AF relaying system for both fixed gain and CSI-assisted relaying systems where the RF link used the spectrum of a PN in the underlay spectrum-sharing strategy. The RF links were experiencing i.n.i.d. Nakagami-m fading, while the FSO link was effected by DGG atmospheric turbulence and pointing error as well. We have considered two strategies for the RF transmitter's power: 1) a single power constraint strategy that considers the interference temperature of the PU and 2) a two power constraints strategy where the interference temperature of the PU and maximum transmitter power constraint of the SU are considered. New closed-form expressions for the outage probability of fixed gain and CSI-assisted relaying systems were derived. In addition, we have analyzed the asymptotic performance and derived diversity and coding gains. More specifically, the derived diversity order was independent of the primary network and power constraints. The coding gain is impressed by power constraints, the interference channel, and the RF-FSO dual-hop links' parameters as well. Also, the coding gain gap between different power constraint strategies was obtained. We also have investigated the diversity-multiplexing trade-off of this network. It has been proved that this trade-off is independent of the primary user and power constraint parameters. We finally point out that the presented results complement and extend several previous results reported in the literature over the past years.

Appendix A

Mathematically speaking, I_2 in Eq. (27) can be written as

$$I_2 = \int_0^\infty \frac{A_1}{\Gamma(m_{SR})\gamma_D} \Upsilon\left(m_{SR}, a_{SR}\frac{\gamma}{\bar{\gamma}_P}\frac{\gamma_D + C}{\gamma_D}\right) \times G_{\alpha_2 p, m}^{m,0}\left[B_1 g^{\alpha_2 p}\left(\frac{\gamma_D}{\mu_r}\right)^{\frac{\alpha_2 p}{r}}\middle| \begin{matrix}\kappa_1 \\ \kappa_2\end{matrix}\right] \mathrm{d}\gamma_D. \tag{A1}$$

For integer values of m_{SR}, we can rewrite the incomplete gamma function as an integral of Eq. (A1) by employing [25], Eq. (8.352.1). Using [34], Eq. (8.4.3.2), we can convert the resulting exponential expression $\exp(-C\gamma a_{SR}/\bar{\gamma}_P\gamma_D)$ to the Meijer G-function as $G_{1,0}^{0,1}[\bar{\gamma}_P\mu_r/C\gamma a_{SR}|1]$. Finally, by employing [34], Eq. (2.24.1.1), we get Eq. (28). The integral expression I_3 in Eq. (27) is obtained as

$$I_3 = \sum_{n=0}^{m_{SR}-1} \frac{1}{n!}\frac{(a_{SR}\gamma)^n \bar{\gamma}_Q^{m_{SP}}}{(a_{SP}\bar{\gamma}_Q + a_{SR}\gamma)^{m_{SP}+n}} \times \int_0^\infty \frac{(\gamma_D + C)^n \gamma_D^{m_{SP}-1}}{\left(\gamma_D + \frac{a_{SR}C\gamma}{a_{SP}\bar{\gamma}_Q + a_{SR}\gamma}\right)^{m_{SP}+n}} \times \Gamma\left(m_{SP}+n, \frac{\bar{\gamma}_Q}{\bar{\gamma}_P}\left(a_{SR}\frac{\gamma}{\bar{\gamma}_Q}\frac{\gamma_D + C}{\gamma_D} + a_{SP}\right)\right) \times G_{\alpha_2 p, m}^{m,0}\left[B_1 g^{\alpha_2 p}\left(\frac{\gamma_D}{\mu_r}\right)^{\frac{\alpha_2 p}{r}}\middle| \begin{matrix}\kappa_1 \\ \kappa_2\end{matrix}\right] \mathrm{d}\gamma_D. \tag{A2}$$

For the integral in Eq. (A2), by using [34], Eq. (8.4.2.5), we can represent the fractional expression in terms of the Meijer G-function as

$$\left(\frac{a_{SP}\bar{\gamma}_Q + a_{SR}\gamma}{a_{SR}C\gamma}\gamma_D + 1\right)^{m-n-m_{SP}} = \frac{1}{\Gamma(m_{SP}+n-m)} G_{1,1}^{1,1}\left[\frac{a_{SP}\bar{\gamma}_Q + a_{SR}\gamma}{a_{SR}C\gamma}\gamma_D\middle| \begin{matrix} m-n-m_{SP}+1 \\ 0 \end{matrix}\right]. \tag{A3}$$

By assuming integer values of m_{SP}, [25], Eq. (8.352.2), and [25], Eq. (1.111), we can expand binomial expressions. Finally, we have an integration on the product of three Meijer G-functions. By using [34], Eq. (8.3.1.21), and [37], Eq. (6.2.3), we can transform these Meijer G-functions into Fox H-functions ([38], Eq. (1.2)). This integral is solved in terms of EGBFHFs in [26], Eq. (2.3); as a result, we arrive at Eq. (28).

Acknowledgment

E. Soleimani-Nasab would like to thank the Iran National Science Foundation (INSF) for supporting this research.

References

[1] S. Haykin, "Cognitive radio: Brain-empowered wireless communications," *IEEE J. Sel. Areas Commun.*, vol. 23, no. 2, pp. 201–220, Feb. 2005.

[2] A. Goldsmith, S. A. Jafar, I. Maric, and S. Srinivasa, "Breaking spectrum gridlock with cognitive radios: An information theoretic perspective," *Proc. IEEE*, vol. 97, no. 5, pp. 894–914, May 2009.

[3] S. Arnon, J. R. Barry, G. K. Karagiannidis, R. Schober, and M. Uysal, Eds., *Advanced Optical Wireless Communication*. New York: Cambridge University, 2012.

[4] H. AlQuwaiee, I. S. Ansari, and M.-S. Alouini, "On the performance of free-space optical communication systems over double generalized gamma channel," *IEEE J. Sel. Areas Commun.*, vol. 33, no. 9, pp. 1829–1840, Sept. 2015.

[5] M. Khalighi and M. Uysal, "Survey on free space optical communication: A communication theory perspective," *IEEE Commun. Surv. Tutorials*, vol. 16, no. 4, pp. 2231–2258, June 2014.

[6] K. P. Peppas and C. K. Datsikas, "Average symbol error probability of general-order rectangular quadrature amplitude modulation of optical wireless communication systems over atmospheric turbulence channels," *J. Opt. Commun. Netw.*, vol. 2, no. 2, pp. 102–110, Feb. 2010.

[7] E. Lee, J. Park, D. Han, and G. Yoon, "Performance analysis of the asymmetric dual-hop relay transmission with mixed RF/FSO links," *IEEE Photon. Technol. Lett*, vol. 23, no. 21, pp. 1642–1644, Nov. 2011.

[8] M. Petkovic, A. Cvetkovic, G. Djordjevic, and G. Karagiannidis, "Partial relay selection with outdated channel state estimation in mixed RF/FSO systems," *J. Lightwave Technol.*, vol. 33, no. 13, pp. 2860–2867, July 2015.

[9] G. Djordjevic, M. Petkovic, A. Cvetkovic, and G. Karagiannidis, "Mixed RF/FSO relaying with outdated channel state information," *IEEE J. Sel. Areas Commun.*, vol. 33, no. 9, pp. 1935–1948, Sept. 2015.

[10] I. S. Ansari, F. Yilmaz, and M.-S. Alouini, "Impact of pointing errors on the performance of mixed RF/FSO dual-hop transmission systems," *IEEE Wireless Commun. Lett.*, vol. 2, no. 3, pp. 351–354, June 2013.

[11] H. Samimi and M. Uysal, "End-to-end performance of mixed RF/FSO transmission systems," *J. Opt. Commun. Netw.*, vol. 5, no. 11, pp. 1139–1144, Nov. 2013.

[12] S. Anees and M. R. Bhatnagar, "Performance of an amplify-and-forward dual-hop asymmetric RF/FSO communication system," *J. Opt. Commun. Netw.*, vol. 7, no. 2, pp. 124–135, Feb. 2015.

[13] E. Zedini, I. S. Ansari, and M.-S. Alouini, "Performance analysis of mixed Nakagami-m and gamma–gamma dual-hop FSO transmission systems," *IEEE Photonics J.*, vol. 7, no. 1, pp. 1–20, Feb. 2015.

[14] J. Zhang, L. Dai, Y. Zhang, and Z. Wang, "Unified performance analysis of mixed radio frequency/free-space optical dual-hop transmission systems," *J. Lightwave Technol.*, vol. 33, no. 11, pp. 2286–2293, June 2015.

[15] M. R. Bhatnagar and M. K. Arti, "Performance analysis of hybrid satellite-terrestrial FSO cooperative system," *IEEE Photon. Technol. Lett.*, vol. 25, no. 22, pp. 2197–2200, Nov. 2013.

[16] I. S. Ansari, M. M. Abdallah, M.-S. Alouini, and K. A. Qaraqe, "A performance study of two hop transmission in mixed underlay RF and FSO fading channels," in *IEEE Wireless Communication Networking Conf. (WCNC)*, Apr. 2014, pp. 388–393.

[17] I. S. Ansari, M. M. Abdallah, M.-S. Alouini, and K. A. Qaraqe, "Outage performance analysis of underlay cognitive RF and FSO wireless channels," in *Int. Workshop Optical Wireless Communication (IWOW)*, Madeira, Portugal, Sept. 2014, pp. 6–10.

[18] F. S. Al-Qahtani, A. H. Abd El-Malek, I. S. Ansari, R. M. Radaydeh, and S. A. Zummo, "Outage analysis of mixed underlay cognitive RF MIMO and FSO relaying with interference reduction," *IEEE Photonics J.*, vol. 9, no. 2, pp. 1–22, Apr. 2017.

[19] L. Yang, M. Hasna, and I. S. Ansari, "Unified performance analysis for multiuser mixed η-μ and M-distribution dual-hop RF/FSO systems," *IEEE Trans. Commun.*, vol. 65, no. 8, pp. 3601–3613, May 2017.

[20] M. Kashani, M. Uysal, and M. Kavehrad, "A novel statistical channel model for turbulence-induced fading in free-space optical systems," *J. Lightwave Technol.*, vol. 33, no. 11, pp. 2303–2312, June 2015.

[21] E. Soleimani-Nasab and M. Uysal, "Generalized performance analysis of mixed RF/FSO cooperative systems," *IEEE Trans. Wireless Commun.*, vol. 15, no. 1, pp. 714–727, Jan. 2016.

[22] J. Feng and X. Zhao, "Performance analysis of mixed RF/FSO systems with STBC users," *Opt. Commun.*, vol. 381, pp. 244–252, Dec. 2016.

[23] A. M. Salhab, F. S. Al-Qahtani, R. M. Radaydeh, S. A. Zummo, and H. Alnuweiri, "Power allocation and performance of multiuser mixed RF/FSO relay networks with opportunistic scheduling and outdated channel information," *J. Lightwave Technol.*, vol. 34, no. 13, pp. 3259–3272, July 2016.

[24] A. H. Abd El-Malek, A. M. Salhab, S. A. Zummo, and M. Alouini, "Security-reliability trade-off analysis for multiuser SIMO mixed RF/FSO relay networks with opportunistic user scheduling," *IEEE Trans. Wireless Commun.*, vol. 15, no. 9, pp. 5904–5918, May 2016.

[25] I. S. Gradshteyn and I. M. Ryzhik, *Table of Integrals, Series and Products*, A. Jeffrey, Ed., 7th ed. San Diego: Elsevier, 2007.

[26] P. K. Mittal and K. C. Gupta, "An integral involving generalized function of two variables," *Proc. Indian Acad. Sci. A*, vol. 75, no. 3, pp. 117–123, Mar. 1972.

[27] T. Q. Duong, D. B. da Costa, M. Elkashlan, and V. N. Q. Bao, "Cognitive amplify-and-forward relay networks over Nakagami-m fading," *IEEE Trans. Veh. Technol.*, vol. 61, no. 5, pp. 2368–2374, June 2012.

[28] T. Q. Duong, D. B. da Costa, T. Tsiftsis, C. Zhong, and A. Nallanathan, "Outage and diversity of cognitive relaying systems under spectrum sharing environments in Nakagami-m fading," *IEEE Commun. Lett.*, vol. 16, no. 12, pp. 2075–2078, Dec. 2012.

[29] M. K. Simon and M.-S. Alouini, *Digital Communication Over Fading Channels*, 2nd ed. New Jersey: Wiley, 2005.

[30] A. Ghasemi and E. S. Sousa, "Fundamental limits of spectrum-sharing in fading environments," *IEEE Trans. Wireless Commun.*, vol. 6, no. 2, pp. 649–658, Feb. 2007.

[31] Q. Zhao, S. Geirhofer, L. Tong, and B. M. Sadler, "Opportunistic spectrum access via periodic channel sensing," *IEEE Trans. Signal Process.*, vol. 56, no. 2, pp. 785–796, Feb. 2008.

[32] A. A. Farid and S. Hranilovic, "Outage capacity optimization for free-space optical links with pointing errors," *J. Lightwave Technol.*, vol. 25, no. 7, pp. 1702–1710, July 2007.

[33] I. S. Ansari, F. Yilmaz, and M.-S. Alouini, "Performance analysis of FSO links over unified gamma–gamma turbulence channels," in *IEEE Vehicular Technology Conf. (VTC Spring)*, Glasgow, Scotland, May 2015, pp. 1–5.

[34] A. P. Prudnikov, Y. A. Brychkov, and O. I. Marichev, *Integrals and Series. Volume 3: More Special Functions*. Florida: CRC Press, 1999.

[35] Z. Wang and G. B. Giannakis, "A simple and general parameterization quantifying performance in fading channels," *IEEE Trans. Commun.*, vol. 51, no. 8, pp. 1389–1398, Dec. 2003.

[36] H. Lei, I. S. Ansari, G. Pan, B. Alomair, and M. S. Alouini, "Secrecy capacity analysis over α – μ fading channels," *IEEE Commun. Lett.*, vol. 21, no. 6, pp. 1445–1448, June 2017.

[37] M. D. Springer, *The Algebra of Random Variables*. New York: Wiley, 1979.

[38] A. Mathai, R. K. Saxena, and H. J. Haubold, *The H-Function: Theory and Applications*. Springer, 2010.